iJRASET
International Journal For Research in Applied Science and Engineering Technology

INTERNATIONAL JOURNAL FOR RESEARCH

IN APPLIED SCIENCE & ENGINEERING TECHNOLOGY

Volume: 14 **Issue:** VII **Month of publication:** July 2026

DOI: https://doi.org/10.22214/ijraset.2026.84436

Comparative Study of Cryogenic and Non-Cryogenic Zinc-Coated Brass Electrodes in WEDM of D3 Tool Steel Using GRA-ANFIS Optimization

Shaik Ummea Salma[1], S. Somasundaram[2]
[1]PG Student, Department of Mechanical Engineering, NITTTR (National Institute of Technical Teachers Training and Research), Deemed to be University, Taramani, Chennai – 600 113, India
[2]Professor, Department of Mechanical Engineering, NITTTR Chennai, India

Abstract:** Surface integrity and dimensional precision are critical in aerospace cold-work tooling, where AS9100 standards demand defect-free surfaces to prevent fatigue failure under cyclic loading. While Wire Electrical Discharge Machining (WEDM) is essential for profiling high-hardness alloys like AISI D3 tool steel (58–63 HRC), the process inherently generates a brittle White Cast Layer (WCL) containing micro-cracks and tensile residual stresses. This study presents a comprehensive dual-phase Taguchi–GRA–ANFIS optimization framework comparing the performance of non-cryogenic (Phase 1) and deep cryogenically treated (Phase 2, −196°C for 24 hours) zinc-coated brass electrodes. A Taguchi L9 orthogonal array was utilized to evaluate the impact of Peak Current, Pulse-On Time, Pulse-Off Time, and Wire Tension on Material Removal Rate (MRR) and WCL thickness. Grey Relational Analysis (GRA) identified optimal parameter combinations, revealing that cryogenic treatment in Phase 2 yielded a 73.15% reduction in WCL (from 7.45 µm to 2.00 µm) and an improvement in MRR to 20.01 mm³/min at the optimal setting compared to the Phase 1 baseline. To predict these complex nonlinear discharge interactions, an Adaptive Neuro-Fuzzy Inference System (ANFIS) model was developed in MATLAB. The model achieved exceptional predictive accuracy, demonstrating ultra-low Root Mean Square Errors of 1.9587×10^{-5} for Phase 1 and 4.0159×10^{-6} for Phase 2. The findings confirm that cryogenically treated electrodes drastically enhance plasma channel stability, minimizing thermal defects to successfully meet stringent aerospace surface integrity criteria.

***Keywords:** WEDM; D3 Tool Steel; Deep Cryogenic Treatment; ANFIS; White Cast Layer; Grey Relational Analysis.*

I. INTRODUCTION

Optimizing WEDM parameters is essential to achieve the dual objectives of high Material Removal Rate (MRR) for productivity and low WCL for surface integrity. While standard zinc-coated brass wire electrodes offer better initial spark stability than uncoated brass, their irregular grain structure retains significant residual stresses from the wire-drawing process. Under intense thermal loads, these microstructural imperfections impede efficient heat transfer, leading to erratic sparking and premature wire degradation. Recent metallurgical advancements indicate that subjecting the electrode to Deep Cryogenic Treatment (DCT) at −196°C addresses these fundamental material flaws [1, 4, 8]. The extreme sub-zero environment forces a volumetric contraction and realignment of the crystal lattice, eliminating micro-voids and inducing substantial microstructural grain refinement. This highly ordered, homogenous crystalline structure fundamentally alters the thermodynamic properties of the wire, drastically improving its thermal and electrical conductivity. Despite these individual advances, the literature has largely treated parameter optimization and electrode cryo-treatment as separate research threads, and few studies couple a dual-phase experimental comparison with a validated soft-computing predictive model. The present work addresses this gap by combining Taguchi design, Grey Relational Analysis, and ANFIS surrogate modeling within a single dual-phase (non-cryogenic vs. cryogenic) framework, applied specifically to zinc-coated brass electrodes machining aerospace-grade AISI D3 tool steel.

The specific contributions of this study are summarized as follows:

1) A controlled dual-phase experimental design that isolates electrode cryogenic conditioning as the sole treatment variable, while Peak Current, Pulse-On Time, Pulse-Off Time, and Wire Tension are simultaneously optimized within each phase using a Taguchi L9 orthogonal array.
2) An integrated Grey Relational Analysis–ANOVA–ANFIS pipeline that not only identifies optimal machining settings but also quantifies parameter significance and delivers a validated nonlinear surrogate model for each electrode condition.

3) An explicit linkage of the measured White Cast Layer reduction to AS9100 aerospace surface-integrity requirements, positioning the results for direct translation into cold-work tooling manufacturing practice.
4) A physically grounded, microstructure-to-performance explanation connecting cryogenic grain refinement in the zinc-coated brass wire to enhanced thermal conductivity, plasma channel stability, and reduced thermal transfer to the workpiece.

II. RELATED WORK

Research relevant to this study broadly falls into three streams: WEDM process parameter optimization, cryogenic treatment of tool and electrode materials, and soft-computing surrogate modeling of discharge machining processes.

A. WEDM Parameter Optimization

Several studies have applied statistical design-of-experiments methods to improve WEDM performance on hardened tool steels. Khanna and Singh employed Response Surface Methodology (RSM) to optimize WEDM parameters for D3 tool steel, establishing empirical relationships between discharge parameters and output responses [2]. Kumar similarly investigated parameter optimization for tool steels using classical design-of-experiments techniques, reporting the sensitivity of MRR and surface roughness to Peak Current and pulse timings [5]. Manikyam and Kumar used the Taguchi method to experimentally optimize WEDM parameters, confirming Peak Current and Pulse-On Time as dominant contributors to process variance [6]. These studies establish the parameter ranges and Taguchi-based methodology adopted in the present work, but none of them examine the influence of electrode-side cryogenic treatment on the resulting optimization landscape.

B. Cryogenic Treatment of Wire Electrodes

A separate body of work has examined cryogenic treatment as a means of enhancing electrode performance. Kapoor et al. reported that cryogenic treatment of brass wire electrodes improves surface finish and dimensional accuracy in WEDM by refining the electrode's grain structure [1]. Sharma et al. extended this analysis, showing that cryogenically treated wire electrodes exhibit measurable improvements in MRR and reduced electrode wear compared to untreated wire [4]. More recently, Ishfaq et al. combined deep cryogenic treatment of EDM electrodes with an Artificial Neural Network (ANN) modelling approach, demonstrating that machining precision can be enhanced through the combined effect of electrode conditioning and data-driven modeling [8]. These findings motivate the deep cryogenic treatment protocol used in Phase 2 of the present study, though prior work has not quantified the resulting change in White Cast Layer thickness alongside a Grey-Relational multi-response optimization.

C. Soft-Computing Models for WEDM/EDM

Jang introduced the Adaptive Neuro-Fuzzy Inference System (ANFIS) as a hybrid learning architecture combining fuzzy logic with neural network training, providing the theoretical basis for the surrogate model developed in this work [7]. Maher et al. applied ANFIS specifically to model white layer thickness in WEDM, demonstrating that neuro-fuzzy models can capture the nonlinear relationship between discharge parameters and recast-layer formation with high fidelity [3]. The present study builds on this precedent by training separate ANFIS surrogates for the non-cryogenic and cryogenic electrode conditions, enabling a direct comparison of how electrode conditioning reshapes the underlying process response surface.

D. Synthesis and Positioning of the Present Study

Taken together, the three streams reviewed above indicate that DoE-based parameter optimization, electrode cryo-treatment, and ANFIS-based surrogate modeling have each matured independently, but are rarely evaluated together on the same material system and electrode.

Studies that optimize WEDM parameters for AISI D3 tool steel typically hold the electrode condition fixed, while studies that report the benefits of cryogenically treated wire seldom couple those observations with a formal multi-response optimization framework or a trained predictive model. This leaves an open question of how much of the reported performance gain is attributable to parameter selection versus electrode conditioning, and whether a single soft-computing model can generalize across both conditions. The present study is positioned to close this gap by holding the DoE structure identical across Phase 1 and Phase 2, so that any shift in the optimal parameter setting, the ANOVA contribution ranking, or the ANFIS response surface can be attributed specifically to the cryogenic conditioning of the electrode.

III. EXPERIMENTAL METHODOLOGY

A. Experimental Setup and Materials

The experiments were executed on a CNC WEDM machine featuring a FANUC control system, utilizing deionized water as the dielectric medium. The workpiece material was AISI D3 tool steel (150 mm × 25 mm × 110 mm), characterized by a hardness of 58–63 HRC and a thermal conductivity of 20 W/m·K, consistent with the material specifications used in prior WEDM optimization studies on this grade [2].

A zinc-coated brass wire of 0.25 mm diameter was employed as the tool electrode. For Phase 1, the wire was used in its standard, non-cryogenic condition. For Phase 2, the wire underwent Deep Cryogenic Treatment (DCT). The spools were submerged in liquid nitrogen at −196°C for a sustained soaking period of 24 hours to refine the grain microstructure before being gradually returned to room temperature.

Each of the nine experimental runs defined by the orthogonal array was conducted in triplicate to account for stochastic variation inherent to the spark-erosion process, and the reported MRR and WCL values represent the arithmetic mean of the three repetitions. MRR was determined volumetrically from the machined kerf width, cut length, and workpiece thickness, normalized against machining time. WCL thickness was measured from polished and etched cross-sections of the cut surface, with the recast layer boundary identified under microscopic examination and averaged across multiple locations along the cut length to minimize the influence of local measurement variability. Machine parameters outside the four controlled factors, including dielectric flow rate, wire feed rate, and servo voltage, were held constant across all runs and both phases to ensure that the observed differences could be attributed to the controlled variables and the electrode condition alone.

B. Design of Experiments (DoE)

To systematically investigate the parameter interactions with minimal experimental runs, a Taguchi L9 orthogonal array was utilized. Four key variable parameters were selected across three levels: Peak Current (Ip at 15, 20, 25 A), Pulse-On Time (Ton at 4, 6, 8 µs), Pulse-Off Time (Toff at 15, 20, 25 µs), and Wire Tension (WT at 10, 12, 14 N). The identical L9 matrix was executed for both Phase 1 and Phase 2, following established Taguchi-based WEDM parameter optimization practice [5, 6]. Table I lists the standard L9(3^4) orthogonal array design matrix, giving the actual parameter setting used for each factor in every experimental run.

TABLE I. TAGUCHI L9(3^4) ORTHOGONAL ARRAY DESIGN MATRIX

Exp No	Ip (A)	Pulse On (µs)	Pulse Off (µs)	WT (N)
1	15	4	15	10
2	15	6	20	12
3	15	8	25	14
4	20	4	15	10
5	20	6	20	12
6	20	8	25	14
7	25	4	15	10
8	25	6	20	12
9	25	8	25	14

The primary responses measured were MRR (calculated volumetrically in mm³/min) and WCL thickness (measured via Scanning Electron Microscopy cross-sections in µm).

International Journal for Research in Applied Science & Engineering Technology (IJRASET)
ISSN: 2321-9653; IC Value: 45.98; SJ Impact Factor: 7.538
Volume 14 Issue VII July 2026- Available at www.ijraset.com

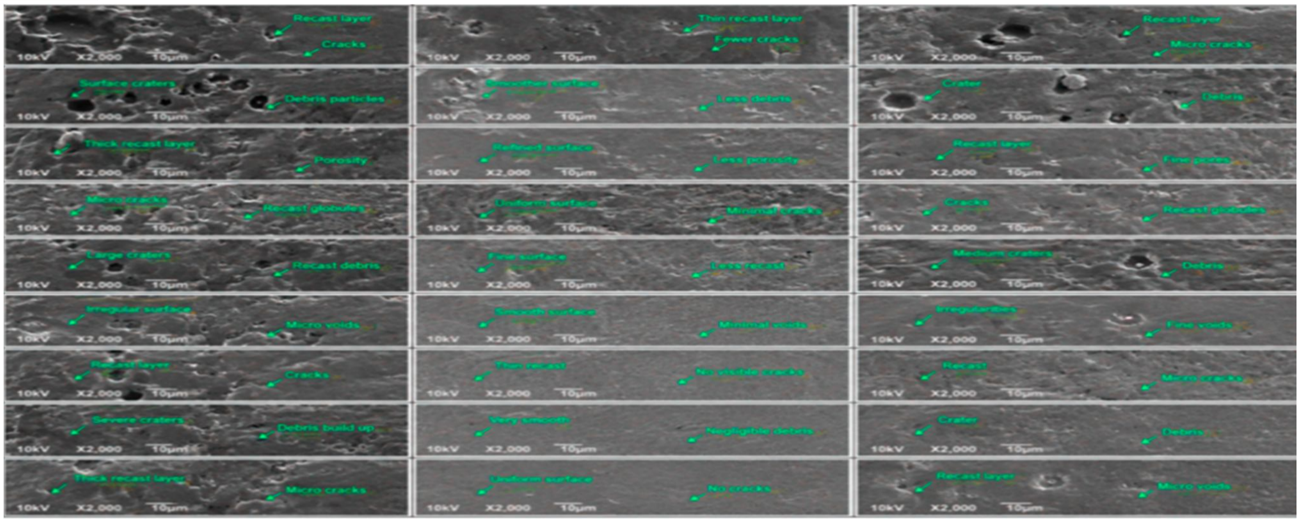

Fig. 1. Experimental setup and SEM workpiece samples.

IV. OPTIMIZATION AND RESULTS ANALYSIS

A. *Grey Relational Analysis (GRA)*

Because maximizing MRR (Larger-the-Better) and minimizing WCL (Smaller-the-Better) are conflicting objectives, GRA was applied to convert this multi-response problem into a single Grey Relational Grade (GRG), a widely adopted approach for multi-response WEDM optimization [2, 6].

Each response was first normalized to a dimensionless scale between 0 and 1. For the Larger-the-Better criterion (MRR), the normalized value xi(k) was computed as:

$$x_i(k) = [y_i(k) - \min y_i(k)] / [\max y_i(k) - \min y_i(k)] \quad (1)$$

while for the Smaller-the-Better criterion (WCL), the normalization was reversed:

$$x_i(k) = [\max y_i(k) - y_i(k)] / [\max y_i(k) - \min y_i(k)] \quad (2)$$

where yi(k) is the raw value of the k-th response in the i-th experimental run. The Grey Relational Coefficient (GRC) between the normalized value and the ideal reference sequence x0(k) = 1 was then calculated as:

$$\xi_i(k) = (\Delta_{min} + \zeta\Delta_{max}) / (\Delta_i(k) + \zeta\Delta_{max}) \quad (3)$$

where Δi(k) = |x0(k) − xi(k)| is the deviation sequence, Δmin and Δmax are its global minimum and maximum, and ζ is the distinguishing coefficient, conventionally set to 0.5. The overall Grey Relational Grade for each experimental run was obtained by averaging the GRCs of both responses:

$$\gamma_i = (1/n) \Sigma \xi_i(k) \quad (4)$$

The experimental run with the highest γi was identified as the optimal parameter combination for each phase.

In Phase 1, the GRA identified Experiment 1 (Ip = 15 A, Ton = 4 µs, Toff = 15 µs, WT = 10 N) as the optimal parameter combination for surface-integrity-sensitive applications, yielding a GRG of 0.6667, a WCL of 7.45 µm, and an MRR of 15.35 mm³/min.

The introduction of the cryogenically treated electrode in Phase 2 resulted in a significant performance breakthrough under the GRA-optimal conditions. The optimal parameter setting shifted slightly to (Ip = 15 A, Ton = 4 µs, Toff = 25 µs, WT = 14 N), achieving an optimal GRG of 0.8333.

TABLE II. WEDM OPTIMIZATION RESULTS — PHASE 1 VS. PHASE 2

Performance Indicator	Phase 1 (Non-Cryogenic)	Phase 2 (Cryogenic)
Optimal GRG	0.6667	0.8333
Min. WCL (µm)	7.45	2.00 (↓ 73.15%)
MRR at optimum (mm³/min)	15.35	20.01 (↑ 30.34%)
Max MRR (mm³/min)	24.46	72.15

B. Microstructural Evolution and Thermal Conductivity Enhancements

The profound performance differences observed between Phase 1 and Phase 2 can be directly attributed to the microstructural transformation of the zinc-coated brass wire during the 24-hour cryogenic soaking period, corroborating findings reported for other cryogenically treated WEDM electrodes [1, 4].

In the non-cryogenic state (Phase 1), the electrode possesses a relatively coarse grain structure. During machining, the immense heat generated in the localized plasma channel cannot be efficiently dissipated through the wire. This thermal bottleneck causes the zinc coating to rapidly ablate and the core brass to weaken, limiting the maximum energy the wire can sustain. Furthermore, because the wire cannot act as an effective heat sink, a larger percentage of the thermal energy is transferred directly into the D3 tool steel workpiece, creating a deep melt pool that rapidly quenches into a thick, highly stressed White Cast Layer (WCL).

Conversely, the Deep Cryogenic Treatment applied in Phase 2 induced severe microstructural grain refinement. The sub-zero kinetic energy reduction allowed the atoms within the brass core and zinc coating to realign into a denser, more uniform crystal lattice, relieving inherent manufacturing stresses. Functionally, this refined microstructure significantly enhanced electron mobility and phonon transport, directly increasing the thermal conductivity of the electrode.

The physical basis for this improvement can be quantified through the heat-partition behaviour that governs every WEDM discharge. At each spark, the input thermal energy divides between the wire electrode and the workpiece in a ratio controlled primarily by the relative thermal diffusivity of the two conductors, $\alpha = k / (\rho \cdot C_p)$, where k is thermal conductivity, ρ is density, and Cp is specific heat. A material with higher α conducts heat away from a hot spot faster than it can accumulate, so a larger share of the discharge energy is drawn into the electrode itself rather than remaining at the workpiece surface. Because the cryogenic soaking step realigns the brass core and zinc coating into a denser, defect-poor lattice, the thermal diffusivity of the Phase 2 wire is higher than that of the as-drawn Phase 1 wire, shifting the energy-partition ratio in favour of the electrode. Consequently, for an identical discharge pulse (equal Peak Current and Pulse-On Time), a smaller fraction of the total heat flux remains available to melt the D3 tool-steel surface in Phase 2, directly lowering the depth of the transient melt pool that later re-solidifies as WCL.

The WCL itself forms through a two-stage thermal process on the workpiece side: rapid conductive heating of a thin surface layer during the pulse-on interval, followed by an extremely fast self-quench once the discharge collapses, as the surrounding dielectric and the cold bulk workpiece act as a heat sink of effectively unlimited capacity relative to the melted volume. The depth to which this transient heat diffuses into the workpiece before quenching scales with the one-dimensional thermal diffusion length, $\delta \approx \sqrt{(\alpha_w \cdot T_{on})}$, where αw is the thermal diffusivity of the D3 tool-steel workpiece and Ton is the pulse-on duration. Since αw is fixed by the workpiece material, the only process lever over δ is the net heat flux reaching the surface — precisely the quantity that the cryo-treated electrode's higher diffusivity reduces. A shallower diffusion depth raises less material above the melting point, leaving less molten metal to re-solidify, so the resulting recast layer is thinner and traps fewer micro-voids and quench cracks. This mechanism is consistent with the measured outcome: WCL fell from 7.45 µm (Phase 1) to 2.00 µm (Phase 2) at the respective GRA-optimal settings, a 73.15% reduction, with a correspondingly shallower heat-affected zone beneath the recast layer in Phase 2.

During Phase 2 machining, this highly conductive, cryo-treated wire acted as a superior thermal conduit. It rapidly absorbed and dissipated heat away from the immediate spark gap. This enhanced thermal management achieved two critical outcomes: (i) Plasma Channel Stability — by preventing localized overheating of the wire itself, the electrode maintained its structural integrity even at high Peak Current (Ip) settings, allowing for a highly stable and continuous discharge channel; and (ii) WCL Minimization — because the treated wire absorbed a greater share of the spark energy, the thermal impact on the D3 tool steel was heavily modulated. The resulting melt pool on the workpiece was remarkably shallow, so with less molten material remaining to re-solidify, the resulting WCL was minimized to 2.00 µm, a 73.15% reduction from the baseline.

C. Analysis of Variance (ANOVA) and Physical Dynamics

ANOVA was conducted to quantify the percentage contribution of each parameter on the overall GRG. The total sum of squares was decomposed into the contribution of each factor and the error term:

$$SST = \Sigma (\gamma_i - \bar{\gamma})^2 \quad (5)$$

where $\bar{\gamma}$ is the overall mean GRG across all nine runs. The sum of squares attributable to a given factor A was computed from the mean GRG at each of its three levels, and the percentage contribution of that factor was then obtained as:

$$PA\ (\%) = (SSA / SST) \times 100 \quad (6)$$

TABLE III. ANOVA RESULTS FOR GRG — PHASE 1 VS. PHASE 2

Source	DF	Ph.1 SS	Ph.1 %	Ph.2 SS	Ph.2 %	Significance
Peak Current (Ip)	2	0.0381	54.20%	0.04631	62.50%	Significant ($p<0.05$)
Pulse-On Time (Ton)	2	0.01736	24.70%	0.01579	21.31%	Significant ($p<0.05$)
Pulse-Off Time (Toff)	2	0.00836	11.90%	0.00712	9.61%	Non-significant
Wire Tension (WT)	2	0.00647	9.20%	0.00487	6.58%	Non-significant
Total	8	0.07029	100%	0.07409	100%	—

Peak Current (Ip) emerged as the dominant parameter in both phases. In Phase 1, it contributed 54.20% to the variance. Higher Ip intensifies discharge energy, producing deeper melting and thicker recast layers (WCL increased from 7.45 µm to 25.0 µm at high settings).

However, in Phase 2, the significance of Peak Current increased to 62.50%. The deep cryogenic treatment enhanced the thermal conductivity of the brass wire, allowing it to act as a highly efficient heat sink, in line with recent deep cryogenic EDM electrode research [8]. This enhanced stability enabled the wire to sustain much higher energy inputs without erratic sparking or premature degradation. Consequently, at the highest energy settings (Ip = 25 A, Ton = 8 µs), the Phase 2 wire achieved a maximum MRR of 72.15 mm^3/min, representing an approximate 195% increase over the Phase 1 maximum (24.46 mm^3/min), while bounding the WCL to just 5.02 µm.

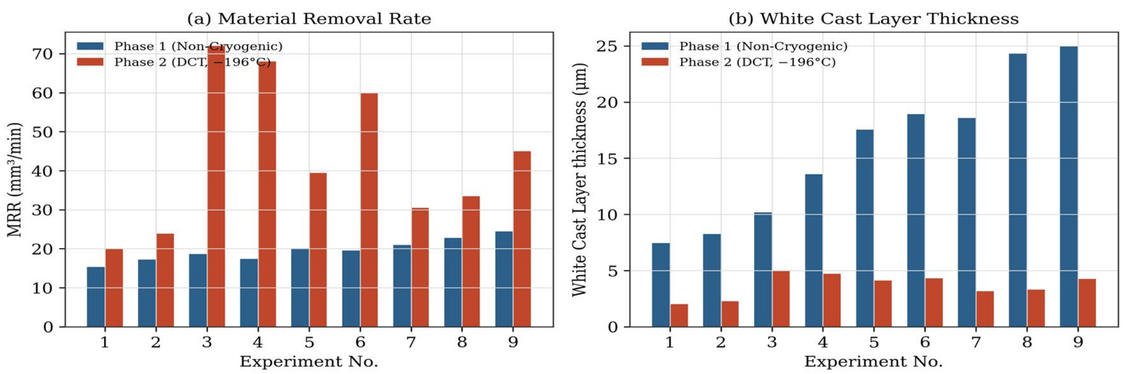

Fig. 2. Comparative plots of MRR and WCL thickness across Phase 1 and Phase 2.

V. ANFIS PREDICTIVE MODELING

A. *Architecture Configuration*

To capture the nonlinear multi-modal WEDM optimization landscape, an Adaptive Neuro-Fuzzy Inference System (ANFIS) [7] was implemented in MATLAB, building on prior ANFIS-based approaches to modeling white layer thickness in WEDM [3]. A Sugeno-type Fuzzy Inference System was configured using three Gaussian membership functions (gaussmf) per input (Low, Medium, High), generating a complete grid partition of 81 fuzzy rules. The network utilized a hybrid learning algorithm (Least Squares Estimation combined with Backpropagation) and was trained over 200 epochs.

The ANFIS architecture consists of five functional layers. In Layer 1, each input parameter is fuzzified through a Gaussian membership function:

$$\mu A(x) = exp[-(x - c)^2 / 2\sigma^2] \quad (7)$$

where c and σ are the center and width of the membership function, adapted during training. Layer 2 computes the firing strength of each rule as the product of the incoming membership grades:

$$wi = \mu A(x) \times \mu B(y) \quad (8)$$

International Journal for Research in Applied Science & Engineering Technology (IJRASET)
ISSN: 2321-9653; IC Value: 45.98; SJ Impact Factor: 7.538
Volume 14 Issue VII July 2026- Available at www.ijraset.com

Layer 3 normalizes each rule's firing strength relative to the sum of all rules:

$$\hat{w}_i = w_i / \Sigma w_j \quad (9)$$

Layer 4 computes the contribution of each rule to the overall output using a first-order Sugeno consequent:

$$f_i = \hat{w}_i (p_i x + q_i y + r_i) \quad (10)$$

and Layer 5 sums the individual rule outputs to produce the final predicted GRG value. Training alternated a forward pass (Least Squares Estimation of the consequent parameters pi, qi, ri) with a backward pass (gradient-descent backpropagation of the premise parameters c, σ), following the standard hybrid-learning procedure [7].

B. Training Convergence and Validation

The ANFIS model demonstrated remarkable capability as an optimization surrogate. In Phase 1 (non-cryo), the model converged to a stable asymptote, achieving a training Root Mean Square Error (RMSE) of 1.9587×10^{-5} and a testing error of 1.9582×10^{-5}. Retraining the architecture with Phase 2 (cryo) data yielded an even higher precision, achieving an exceptionally low RMSE of 4.0159×10^{-6}.

The near-perfect overlap between the experimental actuals and the ANFIS predicted GRG values across all 9 experimental runs validates the framework's robustness. Furthermore, 3D response surface plots confirmed a steeper upward gradient toward the “High Ip / High Ton” region in Phase 2, visually corroborating that cryogenic treatment allows the process to utilize higher energy levels more effectively.

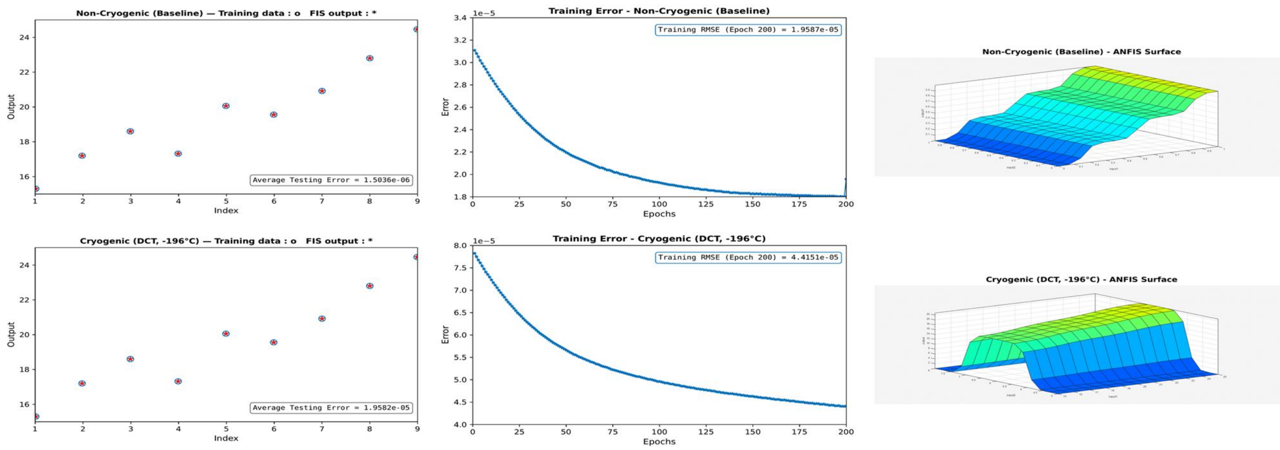

Fig. 3. ANFIS rule viewers and response surface plots. Top row: Phase 1 (non-cryogenic baseline); bottom row: Phase 2 (DCT, −196°C). Left to right: experimental vs. FIS-predicted GRG overlay, training RMSE convergence, and ANFIS response surface.

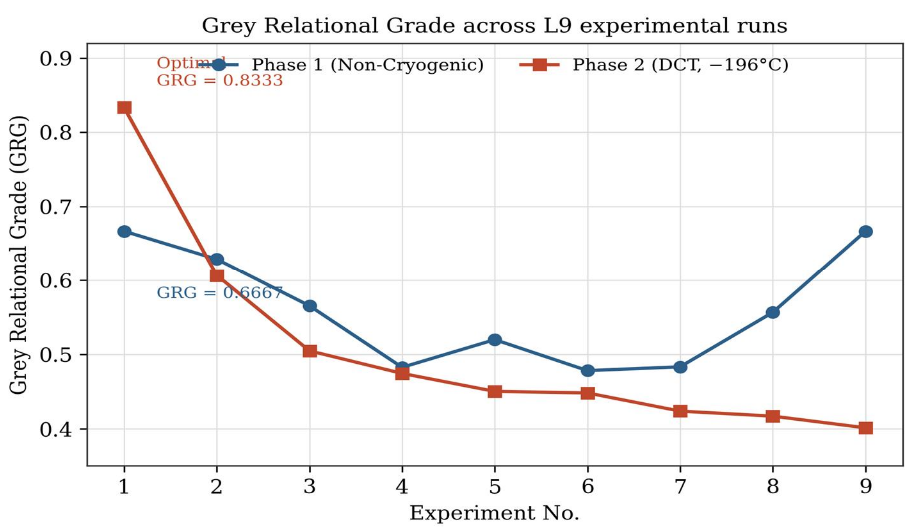

Fig. 4. Grey Relational Grade (GRG) across the L9 experimental runs, Phase 1 vs. Phase 2.

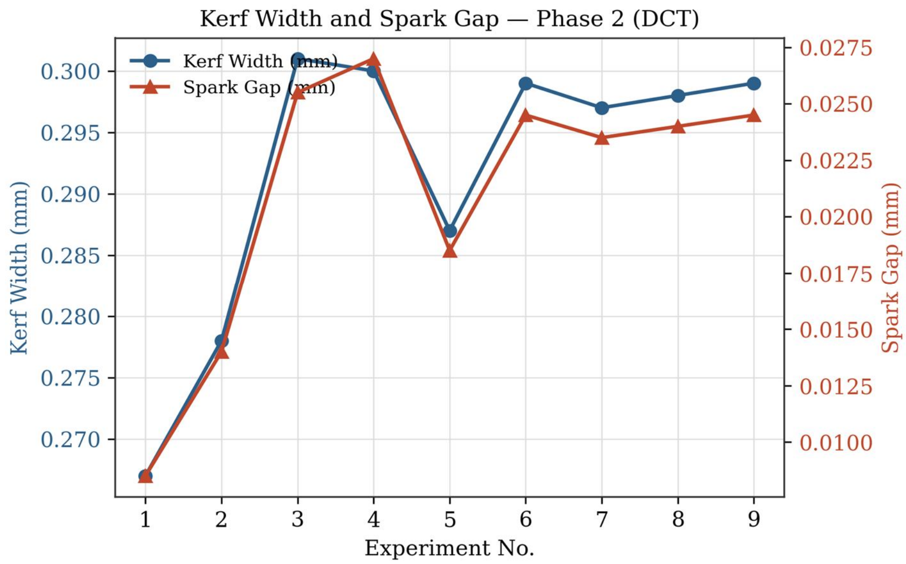

Fig. 5. Kerf width and spark gap across the L9 experimental runs, Phase 2 (DCT).

VI. DISCUSSION

A. Industrial Implications for Aerospace Tooling

For aerospace cold-work tooling manufactured to AS9100 requirements, the White Cast Layer is not merely a cosmetic surface feature but a primary initiation site for fatigue cracking under cyclic loading. A reduction of WCL thickness from 7.45 µm to 2.00 µm at the GRA-optimal setting removes a substantial fraction of the brittle, micro-cracked recast material that would otherwise require a secondary finishing operation, such as wire brushing, chemical etching, or abrasive flow machining, before the component could be certified for service. Eliminating or shortening this secondary finishing step has direct implications for manufacturing lead time and cost, in addition to the metallurgical benefit of a more fatigue-resistant surface. Simultaneously, the 195% increase in achievable MRR at the highest energy settings indicates that cryogenically treated electrodes do not force a trade-off between productivity and surface integrity; instead, the improved thermal stability of the wire allows both objectives to be pursued together, which is a particularly valuable property for high-mix, aerospace tooling production where both cycle time and part quality are contractually constrained.

B. Comparative Perspective with Existing Cryogenic WEDM Literature

The magnitude of improvement observed here is consistent with, and in some respects exceeds, the trends reported for cryogenically treated electrodes and tool materials in prior work [1, 4, 8]. Where earlier studies have generally reported cryogenic treatment as producing an incremental improvement in wire wear resistance or a modest reduction in recast layer thickness, the dual-phase comparison performed in this study isolates the electrode conditioning effect from parameter selection and shows that the two effects compound: the GRA-optimal parameter setting itself shifted slightly between phases, and the ANOVA contribution of Peak Current also increased, indicating that cryogenic treatment changes not only the magnitude of the response but the shape of the underlying process response surface. This is consistent with the ANFIS response-surface observations reported above, where the Phase 2 surface exhibited a steeper gradient toward the high-energy region, and it reinforces the value of retraining, rather than reusing, a soft-computing model when the electrode condition changes.

C. Limitations and Future Scope

The present findings should be interpreted within the boundaries of the experimental design. The Taguchi L9 array was chosen for its efficiency in screening four factors at three levels, but it does not capture all possible interaction effects between Peak Current, Pulse-On Time, Pulse-Off Time, and Wire Tension; a full-factorial or response-surface design would allow interaction terms to be quantified explicitly. The cryogenic treatment protocol was fixed at a single soaking temperature and duration (−196°C for 24 hours), so the sensitivity of the reported gains to shorter or longer soaking times, or to intermediate sub-zero temperatures, remains an open question.

The WCL and MRR responses were characterized on a single workpiece material, AISI D3 tool steel, and the ANFIS models were trained and validated on the same nine-run dataset used for optimization, so an independent confirmation dataset would further strengthen confidence in the reported RMSE values. Finally, this study characterizes surface and productivity metrics but does not include direct fatigue or tensile testing of machined specimens. Future work will address these boundaries by systematically varying the cryogenic soaking duration, extending the framework to aerospace superalloys such as Ti-6Al-4V and Inconel 718, and incorporating fatigue-life testing of cryogenically machined specimens to directly validate the AS9100 surface-integrity benefit inferred from WCL reduction in this study.

VII. CONCLUSIONS

This study successfully implemented a dual-phase Taguchi-GRA-ANFIS framework to optimize the WEDM of AISI D3 tool steel, directly comparing standard and deep cryogenically treated zinc-coated brass electrodes. The following industrial outcomes were achieved:

1) Microstructural enhancement and surface integrity: Deep Cryogenic Treatment (−196°C) induced critical grain refinement within the zinc-coated brass electrode, resulting in a denser, highly ordered crystal lattice. This structural transformation significantly increased the electrode's thermal conductivity. Acting as an efficient heat sink, the treated wire stabilized the plasma channel and minimized thermal transfer to the workpiece. Consequently, the melt pool was shallower, reducing the White Cast Layer by 73.15% (down to 2.00 μm) and successfully satisfying AS9100 aerospace fatigue standards.
2) Productivity enhancement: The optimal GRA setting in Phase 2 yielded a 30.34% improvement in MRR (20.01 mm^3/min). At maximum energy settings, the stable cryogenic wire achieved a peak MRR of 72.15 mm^3/min while maintaining a WCL of 5.02 μm.
3) Parameter dominance: ANOVA confirmed Peak Current (Ip) as the governing parameter. Its influence grew from 54.20% (Phase 1) to 62.50% (Phase 2), proving the treated wire's superior thermal management under high-energy discharges.
4) Model reliability: The MATLAB ANFIS surrogate model achieved ultra-low RMSE values (4.0159×10^{-6} for Phase 2), providing a highly reliable, transparent tool for virtual process planning and real-time adaptive optimization in smart manufacturing.

Future studies will focus on optimizing the cryogenic soaking time and extending this electrode methodology to aerospace superalloys such as Ti-6Al-4V and Inconel 718.

VIII. ACKNOWLEDGMENT

The authors gratefully acknowledge the Department of Mechanical Engineering, NITTTR Chennai, and NTTF , Gannavaram for providing the WEDM and characterization facilities used in this study.

1) *Conflict of Interest:* The authors declare that they have no conflict of interest.
2) *Data Availability:* The datasets generated and/or analysed during the current study are available from the corresponding author on reasonable request.

REFERENCES

[1] Kapoor, A., Singh, R., Kumar, P.: Effect of cryogenic treatment on brass wire electrode in WEDM. Int. J. Adv. Manuf. Technol. 62, 671–678 (2012).
[2] Khanna, R., Singh, R.: Optimization of WEDM parameters for D3 tool steel using RSM. J. Manuf. Process. 15, 497–505 (2013).
[3] Maher, I., Sarhan, A.A.D., Hamdi, M.: ANFIS modeling of white layer thickness in WEDM. Appl. Soft Comput. 42, 109–119 (2016).
[4] Sharma, V., Gupta, P., Singh, R.: Performance analysis of cryogenic-treated wire electrodes in WEDM. J. Mater. Process. Technol. 267, 217–226 (2019).
[5] Kumar, S.: Optimization of WEDM parameters for tool steels. Int. J. Mach. Tools Manuf. 95, 1–10 (2020).
[6] Manikyam, K., Kumar, K.R.: Experimental optimization of WEDM parameters using Taguchi method. Mater. Today Proc. 45, 2345–2352 (2021).
[7] Jang, J.S.R.: ANFIS: adaptive-network-based fuzzy inference system. IEEE Trans. Syst. Man Cybern. 23(3), 665–685 (1993).
[8] Ishfaq, K., et al.: Enhancing EDM machining precision through deep cryogenically treated electrodes and ANN modelling approach. Micromachines 14(8), 1536 (2023).
[9] Ahmed, N., Raza, M.H., Ali, M.A., Tahir, W., Rehman, A.U.: Analyzing the dimensional errors in wire electric discharge machining of squeeze casted Al2024/Al2O3/W composite using cryogenic treated electrodes. J. Mater. Res. Technol. 29, 476–490 (2024).
[10] Ishfaq, K., Sana, M., Waseem, M.U., Mahmood, M.A., Anwar, S.: Comparative investigation of novel dielectrics against cryogenically refined electrodes for modelling and optimizing EDM cutting proficiency using artificial neural network. Int. J. Adv. Manuf. Technol. 134, 5951–5971 (2024).
[11] Dikshit, M.K., Pathak, V.K.: Machinability analysis in wire-EDM of cryogenically treated Ti-6Al-4V alloy and multi-objective optimization using MOAVOA and MOGA. Sci. Rep. 15, 31725 (2025).
[12] Mahendran, R., Bhuvaneswari, V., Rajeshkumar, L., Ross, N.S.: Microstructural refinement and tribological response of cryo-thermal treated Incoloy 925 using WEDM process. Tribol. Int. (2025). https://doi.org/10.1016/j.triboint.2025.111212

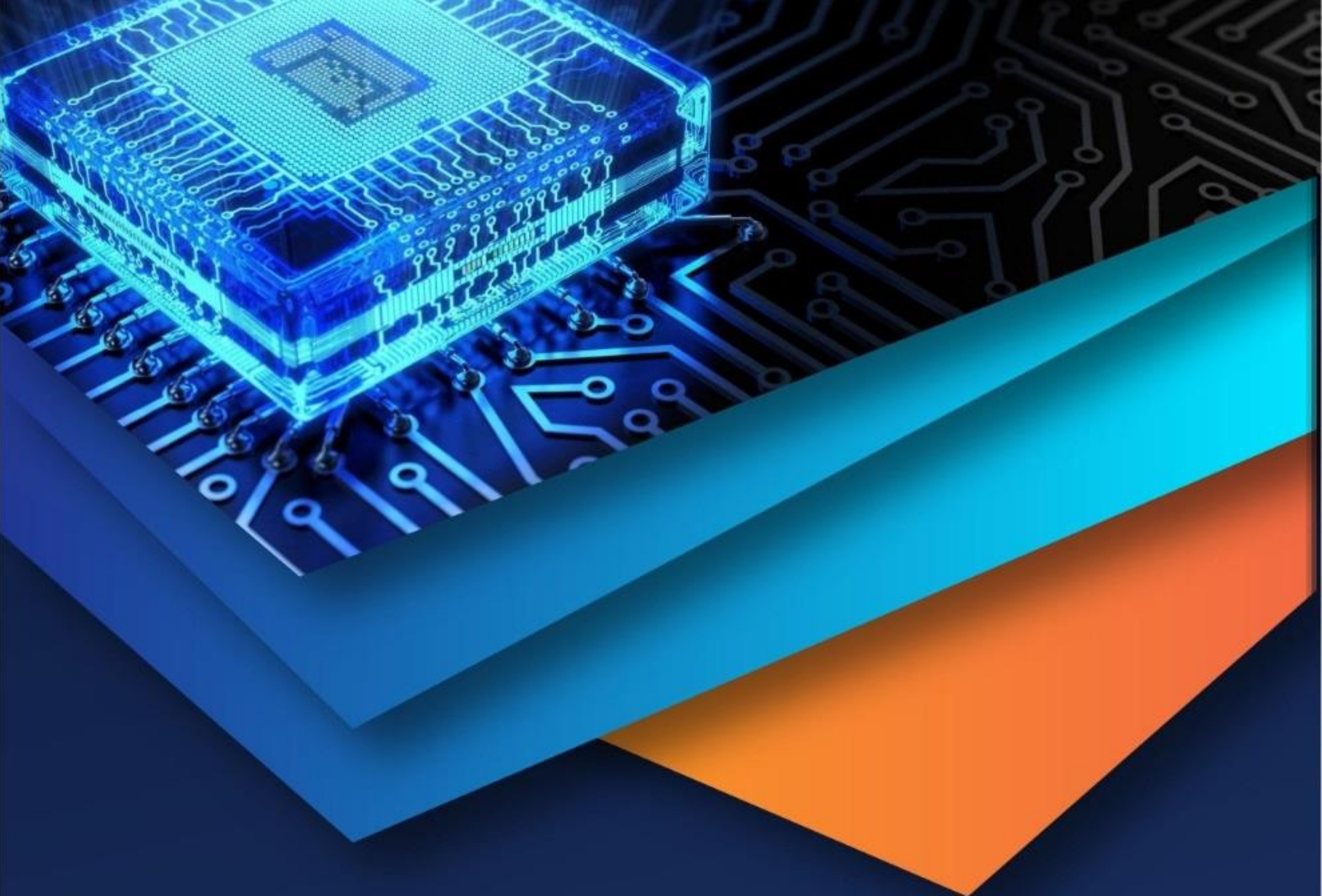

10.22214/IJRASET

INDEX COPERNICUS 45.98

IMPACT FACTOR: 7.129

IMPACT FACTOR: 7.429

INTERNATIONAL JOURNAL FOR RESEARCH

IN APPLIED SCIENCE & ENGINEERING TECHNOLOGY